Received: 20 February 2020 | Revised: 6 May 2020 | Accepted: 8 May 2020 | Published on: 15 June 2020

DOI: 10.1002/joc.6648

RESEARCH ARTICLE

International Journal of Climatology RMetS

Vegetation fire activity and the Potential Fire Index (PFIv2) performance in the last two decades (2001–2016)

Alex S. da Silva[1] | **Flavio Justino**[2] | **Alberto W. Setzer**[3] | **Alvaro Avila-Diaz**[2]

[1]Engineering and Geosciences Institute, Federal University of Western Para, Santarem, Brazil

[2]Agricultural Engineering Department, Federal University of Vicosa, Vicosa, Brazil

[3]Fire Program of the National Institute of Space Research (INPE), Sao Jose dos Campos, Brazil

Correspondence
Alex S. da Silva, Engineering and Geoscience Institute, Federal University of Western Para, Room 422 Tapajos Centre, Santarém, Brazil.
Email: alex.ss@ufopa.edu.br

Funding information
Brazilian National Council for Scientific and Technological Development (CNPq); Minas Gerais Research Foundation (FAPEMIG); Coordination for the Improvement of Higher Education Personnel (CAPES)

Abstract

Fire incidence has been linked to multiple factors such as climate conditions, population density, agriculture, and lightning. Recently, fire frequency and severity have induced health problems and contributed to increase atmospheric greenhouse gases. Based on atmospheric susceptibility to fire, this study evaluates the use of a Potential Fire Index (PFIv2) to identify regions prone to fire development, as demonstrated by the satellite detected-fire in the 2001–2016 interval. It is demonstrated that PFIv2 delivers an efficiency by up to 80% in matching the observed fires from Terra/MODIS satellite. The PFIv2 is also able to reproduce more accurately areas with fire activity with respect to its previous version, the PFI. This better performance is linked to the implementation of parameterization of water pressure deficit and atmospheric stability in the lower troposphere, and a new term to represent the effect of surface temperatures, particularly in mid-latitudes and extra-Tropics. To evaluate the performance of the PFIv2 in more details, its comparison to MODIS burned areas demonstrated correlations values higher than 0.6 over the most susceptible regions such as Africa and South America, slightly lower correlation is found where fire does not primary follows the climate annual cycle, and is dominated by high frequency events. These findings indicate that the PFIv2 can be an important tool for decision makers in predicting the potential for vegetation fires development and fire danger.

KEYWORDS

atmospheric conditions, fire weather, Haines index, MODIS

1 | INTRODUCTION

Vegetation fires in consonance with climate conditions play an important role as disturbance agents affecting the structure and the global distribution of ecosystems (Hollmann *et al.*, 2013). In recent decades, government bodies and social institutions have expressed concerns about the indiscriminate use of fire, because wildfires were prominent in modifying climate conditions in the past, and very likely they will be in the future (Harrison *et al.*, 2007), in particular by inducing changes in the atmospheric concentration of greenhouse gases (Langmann *et al.*, 2009; Leys *et al.*, 2018). For instance, vegetation burnings in Indonesia in 1997 and 1998 represent 25% of total CO_2 emissions associated with combustion of fossil fuels (Page *et al.*, 2002).

Currently, on a global perspective, the highest fire occurrences are between July and October. In the Tropics, this is primarily related to the conversion of natural vegetation to pasture and others agriculture proposes

(Silva *et al*., 2003; Justino *et al*., 2010a). Thus, meteorological factors play a mandatory role in fire occurrences. Nevertheless, there is a lively debate on the importance of anthropogenic and climate forcing in contributing to the ignition of wildfires (Huang *et al*., 2015).

Although the majority of vegetation fires has been observed in the Tropics, the Arctic and the extra-Tropics have, in recent decades, experienced an elevated number of wildfires (Veraverbeke *et al*., 2017; Masrur *et al*., 2018). These regions have been affected by higher temperature and distinct pattern of precipitation, resulting in more vulnerable conditions for wildfire development (Krause *et al*., 2014; Veraverbeke *et al*., 2017). Despite a large effort, questions still exist on climate variability and the magnitude and length of the fire season, on a global perspective. Therefore, additional studies are necessary to disentangle the influence of anthropogenic and natural factors in promoting the fire activity. The understanding and skill to predict wildfire occurrence is essential for planning and implementing necessary measures to predict and mitigate the impacts of wildfire. Modelling the vegetation susceptibility to fire activity is therefore vital.

The state-of-the-art fire modelling applies several parameters that include complex interaction among soil characteristics, carbon allocation, and the moisture content of soil litter (Catchpole, 2002; Archibald *et al*., 2009; Bradstock, 2010). Despite the importance of including these conditions in fire simulations, the large number of factors embedded in this fire modelling approach, increases the co-variability of variables and may hamper a clear determination of the cause of fire and the ecosystem dynamics responses (Scheiter and Higgins, 2009). Although, physically consistent, these models also present a level of uncertainty if applied over regions with lower data coverage (Hickler *et al*., 2006; Warmink *et al*., 2010; Finney *et al*., 2012; Skinner *et al*., 2014).

To alleviate these problems simplified models have been proposed. Van Wagner (1987) proposed the Fire Weather Index (FWI), which currently is a worldwide index. It applies three moisture indices: Fine Fuel Moisture Code (FFMC) representing the moisture content in fine fuels. The Duff Moisture Code (DMC) to parameterize organic material, and the Drought Code (DC) which is a deep layer of compact organic material. The combination of these moisture parameters with a Daily Severity Rating (DSR) delivers the fire behaviour indexes (Williams, 1959; Van Wagner, 1970).

Similarly, the United States National Fire Danger Rating System (NFDRS) was revised with the addition of Keetch-Byram Drought Index (KBDI), to account for weather and climatic conditions in the eastern United States (Burgan, 1988; Andrews and Bradshaw, 1997). Currently, the lightning ignition efficiency algorithm has been included by the United States Wild Land Fire Assessment System (Sopko *et al*., 2016).

Justino *et al*. (2010a) formulated the Potential Weather Fire Index (PFI), a simplified index based on four parameters to predict the fire weather danger in Brazil. The PFI is based on maximum temperature, minimum relative humidity, a drought index and the vegetation characteristics. In the last three decades (1990–present), the PFI has shown efficiency in detecting areas with high vulnerability to the occurrence of fire (satellite detected – hot spots) in South America, Africa, and Caribbean (Justino *et al*., 2010a, 2013).

However, limitations have been found in the PFI to estimate the fire danger in extra-tropical latitudes, thus, modifications on the PFI have been implemented and discussed in the present here. The goal of this study is to provide an evaluation of the global fire activity/distribution between 2001–2016, and introduce and validate a modified version of the Potential Weather Fire Index presented by Justino *et al*. (2010a). It has to be stressed that large regions of Africa, South America, and south Asia, do not collect detailed weather information and fire weather parameters, which should be implemented in fire danger models with high level of complexity. In this sense, the availability of more simplified models that can still adequately reproduce fire susceptibility is desirable.

In our article, Section 2 describes the vegetation and climate data utilised, the modelling formulation, and the validation methods. Sections 3 and 4 discuss the capability of the PFIv2 in reproducing more accurately areas with fire activity with respect to its previous version, the PFI. Concluding remarks and model limitation are described in Section 5.

2 | DATA AND METHODOLOGY

2.1 | Study area

The PFIv2, a modified version of the Potential Weather Fire Index (PFI) proposed by Justino *et al*. (2010a) is applied globally over six sub-regions based on the World Meteorological Organization (WMO) framework: (a) Africa (45°S:36°N; 20°W:60°E); (b) Asia (0:66°N; 60:180°E); (c) South America (60°S:15°N; 90:30°W); (d) Americas and Caribbean (15:66°N; 180:50°W); (e) South-West Pacific (50°S:0; 90:180°E); and (f) Europe (36:66°N; 20°W:60°E). The land cover characteristics as delivered by the vegetation type is based on the International Geosphere-Biosphere Programme (IGBP), as shown in Figure 1a.

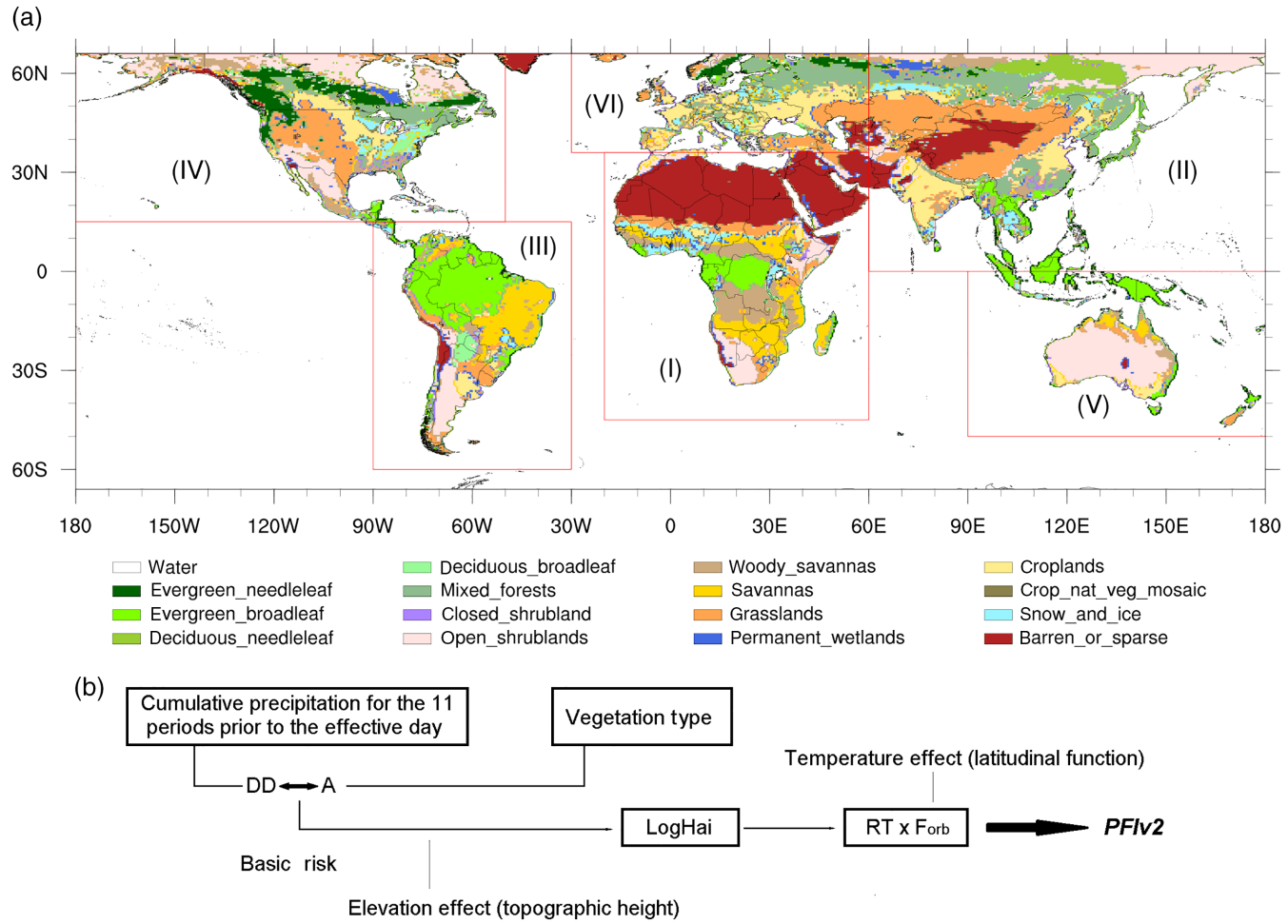

FIGURE 1 (a) Study areas according to the WMO classification, and the vegetation distribution by IGBP (adapted from Friedl *et al.*, 2010). (b) Flowchart presenting the sequence of calculation for the PFIv2 (see text for details)

2.2 | Climate data

The second version of the Potential Fire Index (PFIv2) for the 2001–2016 period, is based on the ERA Interim Reanalysis (Dee *et al.*, 2011), and the CPC Unified Precipitation Project that is underway at NOAA Climate Prediction Center (Xie *et al.*, 2010). The ERA Interim (ERAI) is a global atmospheric reanalysis produced by the European Centre for Medium-Range Weather Forecasts (ECMWF). The ERAI data used in this study are surface temperature, relative humidity and air temperature at 950, 850, 700, and 500 hPa. The spatial resolution of the ERAI is the reduced Gaussian grid N128 (0.75×0.75 latitude $\times$ longitude degree). Since precipitation is the dominant factor in the determining the fire danger in the PFIv2, the application of CPC precipitation contributes to the study because estimates of ERAI precipitation are forecasted and not assimilated. Thus, a double verification of precipitation is necessary because ERAI underestimates precipitation in the Tropics, high- and mid-latitudes, and shows much higher daily variability with respect to the other datasets (Sun *et al.*, 2018).

Several precipitation estimates have been available but all of them exhibit regional limitations. Therefore, we have chosen the CPC as an alternative to ERAI dataset. The CPC includes satellite-rain gauge estimates to reduce systematic error, related to evaporation and aerodynamics effects (Huffman *et al.*, 1997). The CPC spatial resolution is 0.5° latitude and longitude over global land areas. This gauge-based analysis of daily precipitation uses data from over 30,000 weather stations that are collected from multiple agencies. Historical records, independent information from measurements at nearby stations, radar and satellite observations, as well as numerical model forecasts are applied in the quality control of CPC data.

2.3 | Formulation of the Potential Weather Fire Index version 2

The Potential Fire Index version 2 (PFIv2) improves an earlier version proposed by Justino *et al.* (2010a), in which the main assumption is based on accumulated precipitation in distinct time intervals. The PFIv2 is highly correlated with the duration of the dry periods, the type and natural cycle of defoliation of the vegetation, vapour pressure deficit and atmospheric stability at the lower atmosphere.

The PFIv2 reference calculation is the 'Days of Dryness' (DD), which is a hypothetical number of days without precipitation during the last 120 days (Justino *et al.*, 2010a), as described below:

1. Determine for a given geographic area, the value of precipitation, in millimetres (mm) accumulated for the 11 immediately preceding periods of 1, 2, 3, 4, 5, 6–10, 11–15, 16–30, 31–60, 61–90 and 91–120 days.
2. Calculate the 'precipitation factors' (PF) with values ranging from 0 to 1 for each of the 11 periods (see eqs. (1)–(11) in Justino *et al.*, 2010a), using an empirical exponential function of the precipitation in millimetres for each period. Afterwards, as shown by Equation (1) the days of droughts (DD) is computed.

$$\mathrm{DD}=105\times(\mathrm{PF}_1\times\mathrm{PF}_2\cdots\times\mathrm{PF}_{61-90}\times\mathrm{PF}_{91-120}). \quad (1)$$

In fact, the 105 is included in the DD equation to assure that in the situation of no precipitation in the 120 days interval, any kind of vegetation will be dry enough to allow fire occurrence. The 105 has been inferred based on the number of days that might be necessary to evergreen broadleaf or tropical forests allow combustion. The PFIv2 also takes into account the vegetation type and their vulnerability to atmospheric conditions. This is important because savannas and grassland are, for instance, more susceptible to erratic wildfires as compared to evergreen forests. This is defined as the basic risk (BR; Equation (2)):

$$\mathrm{BR}=0.9\times(1+\sin(A\times\mathrm{DD}))/2. \quad (2)$$

The 'A' reproduces fire susceptibility of those 17 original vegetation classes adopted by the IGBP and shown in Figure 1a. The 'A' index is determined based on a combination between the presence of fires and the BR/danger. Initially, is determined the number of DD in the grid box, if the presence of fire is identified the BR/danger should be maximum. Thus, as the variation in the intensity and duration of sunlight throughout the year is sinusoidal, the phenology of vegetation naturally tends to follow the same rhythm. The A value must agree with the relationship between DD and maximum BR/danger, as shown in Justino *et al.* (2010a, 2013). Based on Equation (2), low values of A indicate that the vegetation requires a longer period without precipitation to reach the maximum BR. For instance, regions covered by non-forests experience high BR under 45 days of dryness, whereas areas covered by evergreen forests need 105 days of low precipitation to deliver similar BR. Other feature that must be included in the fire danger is the effect of surface elevation (Tymstra *et al.*, 2010).

The elevation affects the atmospheric characteristics and through changes in surface pressure, due to temperature and humidity of the air, can increase the windward flow, further modifying vegetation health and fuels availability resulting in fire potential. In this sense, a parameter derived from Haines Index (HI) is also included to compute the wildfire danger (see Table 1 in Justino *et al.*, 2010b). This is computed by the combination of the stability (s) and humidity of the air (q) at three atmospheric layers, 900, 850, and 700 hPa (Haines, 1988; Winkler *et al.*, 2007; Potter, 2018). It has to be mentioned that in PFIv2, the HI adds value to improve the fire danger, with other parameters such as precipitation function, vegetation, and surface temperatures. As shown by Potter (2018) the use of HI for a global assessment of fire danger is limited, and does not provide a real fire danger estimation. However, the concept of Haines is very useful to the PFIv2, in particular, by applying the stability and humidity at different atmospheric layers. It is important to note that the first version of the PFI does not take into account the elevation of the surface. This limitation is alleviated in the PFIv2 by including the vertical profile of the atmosphere from surface to 700 hPa. A logistic function is applied because the HI provides discrete values between the atmospheric layers, whereas the PFIv2 follows a continuous function from 0 to 1.

In the PFIv2, the modified HI is represented by the classical Verhulst logistic growth equation (see Equation (3)). The logistic function of the fire danger (LF), which characterizes the (s) and (q) of the air is analytically given by:

TABLE 1 Fire risk (PFIv2) levels

Levels	Minimum	Low	Medium	High	Critical
(0–1)	<0.15	0.15–0.4	0.4–0.7	0.7–0.95	≥0.95

$$\mathrm{LF}=\begin{pmatrix}(i)\ 7\times10^{-5}\times W^3-0.0035\times W^2+0.072\times W-0.26)\\(ii)\ 1\times10^{-4}\times W^3-0.0056\times W^2+0.115\times W-0.53)\\(iii)\ 9\times10^{-5}\times W^3-0.0067\times W^2+0.196\times W-1.89\end{pmatrix} \quad (3)$$

$$\begin{matrix}\{i\} & \text{if } e\leq 1,500\,\text{m},\\ \{ii\} & \text{if } 1,500\,\text{m}<e<3,500\,\text{m},\\ \{iii\} & \text{if } e\geq 3,500\,\text{m},\end{matrix}$$

where W is the sum of the stability and humidity parameters from the Haines Index (°C) and, e stands for the local elevation (m). From now on the LF term stands for the logistic function on Haines Index. Limitations have been noticed on the previous version of the PFI in particular related to temperature threshold in the extra-tropical regions. To reduce this drawback, a new term to characterize the effect of the air temperature is included as $F_T = \mathrm{RT} \times F_{orb}$, $F_T = (0.02 \times T_x + 0.4) \times (0.003 \times |\mathrm{Lat}| + 1)$, where |Lat| is the latitude module and T_x is the daily maximum temperature. F_{orb} is an adjustment factor for temperature at different latitudes. This is included in the PFIv2 because it parameterizes the influence of temperature in the fire danger as $\mathrm{RT} = 0.02T_x + 0.4$. In the PFI original version, RT has been shown to be little efficient in the sub-Tropics and extra-Tropics for latitudes larger than 30°, where surface temperatures are lower with respect to the Tropics. In most cases, the RT reduces the PFI and PFIv2 in the extra/sub-Tropics. Therefore, to differentiate the effect of temperature in distinct regions we have included the effect of latitude.

Finally, the PFIv2 is computed taking into account all parameters as follow:

$$\mathrm{PFIv2} = \mathrm{BR} \times (a2 \times \mathrm{LF} + b) \times (F_T), \quad (4)$$

where $b = 1.3$ and BR is the same as in the PFI (Justino *et al*., 2010a, 2013). The $a2$ is equal to 0.006 and the term $(a2 \times \mathrm{LF} + b)$ takes into account the logistic function (Equation (3)). The sequence of PFIv2 calculations is shown in Figure 1b. It is important to mention that the PFIv2 maintains the same PFI categories, with a scale ranging from 0 (no danger) to 1 (maximum danger of fire occurrence) (Table 1).

Active fires products from the sixth collection of the Moderate Resolution Imaging Spectro-radiometer (MODIS, https://earthdata.nasa.gov/earth-observation-data/near-real-time/firms) are used to verify the capability of the PFIv2 for detecting the most susceptible region for wildfires development, in the 2001–2016 interval.

The validation of the PFIv2 versus satellite-derived hot spots is carried out by checking the percentage of fires located in the high and critical classes of the PFIv2 grid. Evaluation of the wildfire danger based on PFIv2 may be validated with other satellite as well. For instance, GOES and NOAA products can be utilised. The limitation in satellite wildfires detection is mostly related to the fact that these products are not available prior 2000.

3 | RESULTS AND DISCUSSION

3.1 | Temporal variability of global fires

Fires (hot spots) detected by MODIS instruments on-board NASA's Terra and Aqua satellites (Giglio *et al*., 2016), have been classified seasonally during 2001–2016 period, in three different intervals: November–December–January–February (NDJF); March–April–May–June (MAMJ) and; July–August–September–October (JASO). These intervals show the periodic characteristics of minimum, medium and maximum occurrences of fires interannual variability (Figure 2).

Figure 2 shows that the JASO period experiences the highest incidence of fires on a global perspective. In Africa (Figure 2a–c) the highest fire occurrences are from July to February with more than 1 million fires in some years. MAMJ with about 300,000 fires/year represents the low fire season. The highest fire activity in Africa (Figure 2c) is related to burning practices in order to convert natural vegetation into pasture and agricultural purposes (Silva *et al*., 2003). Fire has also been used to produce charcoal and for personal use and increase income. As discussed by Justino *et al*. (2013), the majority of fires occurs under dry conditions in response to the meridional migration of the Intertropical Convergence Zone (ITCZ). Indeed, fires are concentrated in the Sahelian region from December to March, and in subtropical Africa from July to October. Due to the short length of the MODIS time-series may not be appropriated to assume that in the last two decades the number of fires has statistically increased, but regression analysis indicates an upward trend.

Annual fire occurrences in Asia are shown in Figure 2d,f. During NDJF atmospheric conditions in winter reduce the fire occurrences (Figure 2d). Although, the onset of spring fires is noted in eastern China and central Russia (Figure 2e) related to increasing solar insolation, higher temperatures, and likely associated to human action to remove weeds and clear the pasture (Wolfson, 2012; Marlier *et al*., 2013). In southern Asia during the Boreal summer, there is a reduction of fire occurrences (Figure 2f) mostly due to the influence of the Asian monsoon. It is also very interesting that despite the massive

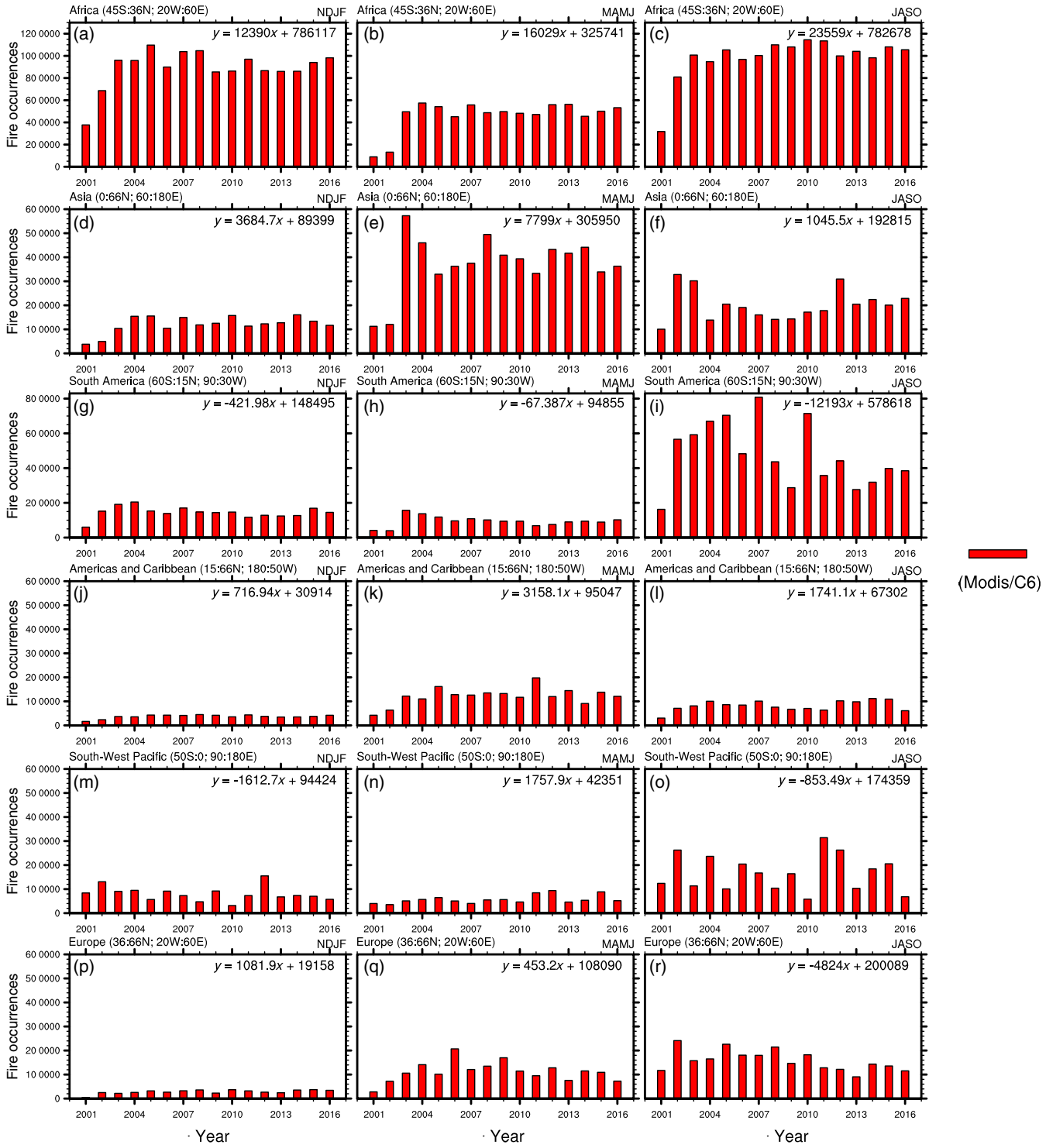

FIGURE 2 Seasonality of fire occurrences detected by Terra/MODIS from 2001 to 2016 for all six study areas. The regression equations are shown in the top right of each annual fire distribution. *Note:* The range values for Africa (a)–(c) and South America (g)–(i) are bigger than that for other regions

amount of rain, the fire activity persists because the large amount of precipitation occurs primarily in southern Asia (Serreze and Barry, 2010), but conditions prone to fires in central and northern Asia are still present.

Turning to the fire distribution in South America (SA), Figure 2g–i show reduced inter-annual fire occurrences from November to June, with respect to the July–October period, because from November to February, the

SA is characterized by higher precipitation induced by the onset of the South American monsoon, the presence of recurrent frontal system and the South Atlantic Convergence Zone (SACZ). During the JASO period (Figure 2i), the central part of Brazil and a large part of the continent experiences very dry conditions. It should also be highlighted that in September and October occur the highest values of surface temperature, and fire activity is maximum.

The inter-annual variability of fires in JASO in SA may be also related to atmospheric conditions induced by the El Niño-Southern Oscillation phenomenon (ENSO). Higher number of hot spots have been detected between 2002 and 2004, in 2007 and 2010. However, it is not clear the direct influence of negative and positive phases of the ENSO because the precipitation response in the continent varies widely (Pereira *et al*., 2014). It should be noted that drought driven by the presence of ENSO can substantially increase the litter/combustible material magnifying the environmental vulnerability for fire occurrence (Silva Junior *et al*., 2019).

According to Figure 2j–l, the incidence of fires in Central, North America and Caribbean are lower from November to February, when the number of hot spots reaches up to 50,000 in the 2001–2016 period (Figure 2k). Turning to the South-West Pacific region, lowest number of fires in the region (Figure 2m–o) takes place from November to June (Figure 2m,n). In opposite, increased fire incidence is noticed in JASO (Figure 2o). Mariani *et al*. (2016) argue that the highest number of fires in Australia, which occurs during the winter–spring season is well correlated to El Niño events. The El Niño has also been claimed to enhance the vegetation susceptibility to fire occurrence in Indonesia (Murdiyarso and Adimingsih, 2007).

Although environmental conditions and vegetation attributes are relatively similar between Europe and North America (Wooster and Zhang, 2004), vegetation burning shows differences in particular from March to October, as shown in Figure 2j,l and p,r. Higher number of hot spots are identified in Europe in October in agreement with warmer and drier conditions.

It is noticed that in Africa, Asia, and North America/Caribbean the number of fires has increased throughout the study interval. However, there is no preferential season, in Africa, the largest increase has been found during JASO, in Asia and North America/Caribbean positive trends are dominant in NDJF. This characteristic is different in South America where negative trends are found. In South-West Pacific and Australia, negative trends are also found from June to February. It has to be stressed that estimates for individual countries may reveal different trends, and that estimates of the number of fires do not reveal the size of burned areas because this issue is related to the severity of the fires.

3.2 | Climatological conditions and the fire danger

Following the evaluation of temporal and regional verification of the hot spots (fires), a discussion on the performance of the proposed fire danger (PFIv2) in reproducing regions with higher fires occurrence is provided. Figure 3a shows the average BR for the JASO interval, in the 2001–2016 period. As a function of precipitation, the BR contributes up to 60% to the final fire danger. It has to be noticed that the CPC precipitation dataset has been used, whereas ERAI is applied for air and dew point temperatures to characterize the atmospheric stability and changes in the water vapour deficit.

Maximum values of BR are noticed in central Eurasia, western North America, southern Africa, Australia, and South America, as a result of dryer conditions related to the lack of precipitation. Interestingly, is that the Haines factor (LogHai, Figure 3b), which takes into account the vertical profile of water vapour matches the BR distribution. This is a response to larger differences of the air and dew-point temperatures in the lower troposphere, which indicates over these regions conditions prone to fire occurrence.

Turning to the temperature factor ($F_{T,}$ Figure 3c), it is demonstrated that the most susceptible regions for fire occurrence are located in the Tropics between 30°S and 30°N. In South America, this might be expected because the Atlantic Subtropical High (ASH) extends towards to the continent, which causes the subsidence of the air and consequently absence of clouds, lack of precipitation, and higher temperatures (Reboita *et al*., 2010; Fetter *et al*., 2018). The combination of these three functions (BR, LogHai, and the F_T) associated to the vegetation pattern (Figure 1) deliver the PFIv2 index.

The PFIv2 reproduces the role of climatic conditions implicit in the method (Figure 3d). For example, the tropical region between 30°N and 30°S is dominated by the contribution of the LogHai factor (atmospheric instability and relative humidity, Figure 3b), in contrasts to lower BR values in response to increased tropical precipitation in particular over the equatorial region in South America and Africa. Even during reduced precipitation intervals these regions may show low values of PFIv2 because the presence of the tropical forest can remove water from subsurface layer, which keep the canopy with considerable level of moisture.

Figure 3d can be used to characterize the influence of vegetation in areas dominated by savannas, pastures,

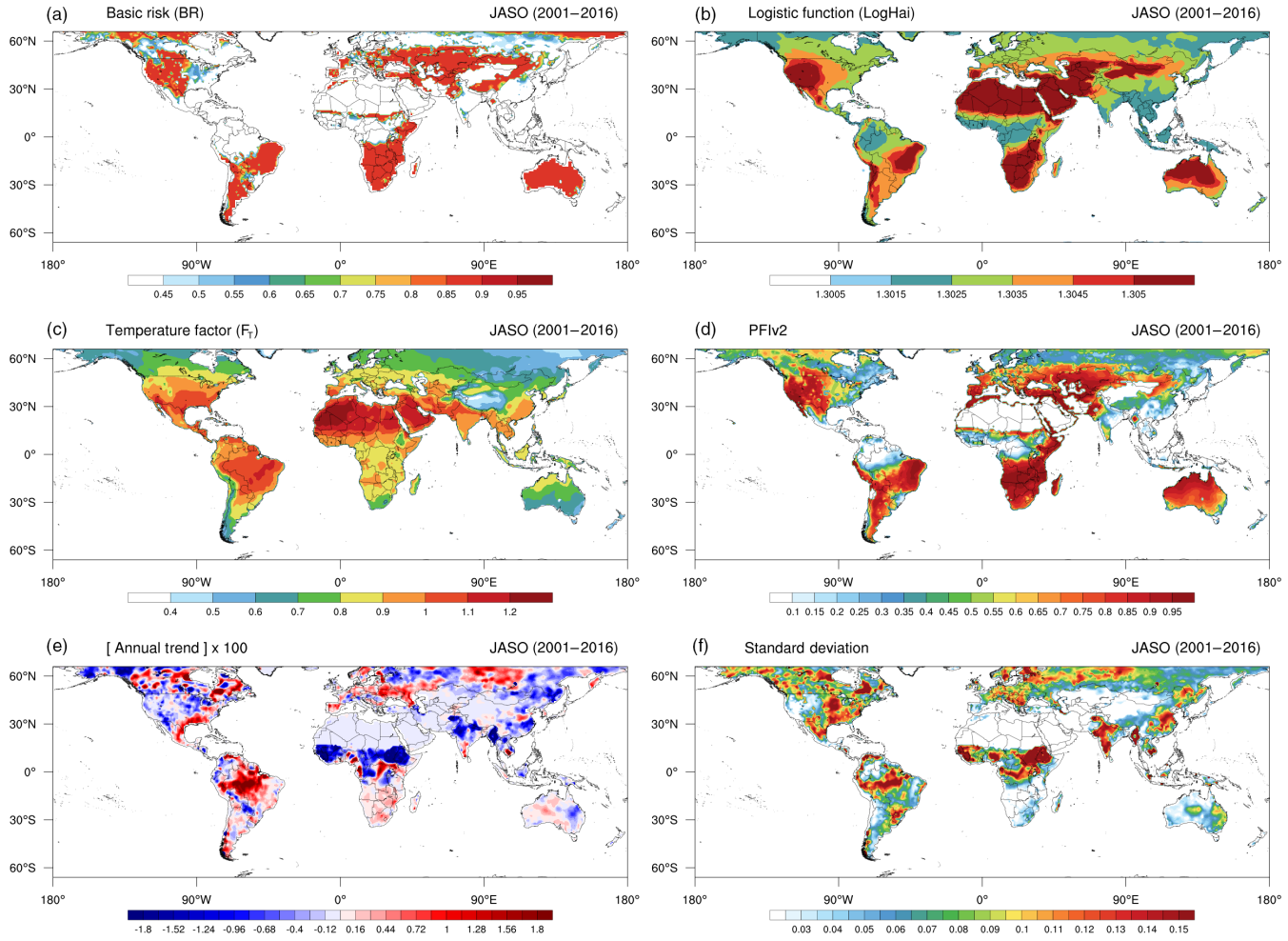

FIGURE 3 Averaged individual PFIv2 factors in July–August–September and October (JASO). (a) Basic risk of fire, (b) fire danger related to the logistic function (LogHai), (c) temperature factor, (d) PFv2, (e) shows the PFIv2 trend in JASO, and (f) shows the PFIv2 *SD*. See Figure 1 for details

grassland, open and closed shrublands. These biomes are associated with increased susceptibility for burning due to the vulnerability of the vegetation to drought conditions and thermal stresses (Anjos and de Toledo, 2018). The effect of vegetation type is also noticed in the eastern part of North America showing low fire danger. Since this region is dominated by deciduous forests, and their dense canopy blocks sunlight to reach the soil, there exists a low amount of combustible material. However, over the west and southwest of the United States the dry atmosphere dominates the fire danger (Figure 3b,d). It has to be mentioned that these regions experience high concentration of cloud-to-ground dry lightning which can induce fires (https://www.wfas.net).

Evaluation to southern Africa revealed that during JASO, the four PFIv2 parameters are in favour of fire occurrence due to low precipitation, dry atmospheric conditions and prone vegetation pattern (savannas and woody savannas). Analyses for Eurasia show that the dominant forcing factor in inducing fire conditions is primary related to the excessive number of days with low precipitation (Figure 3a).

Figure 3e,f shows the JASO annual trends and the *SD* based on global PFIv2 for the 2001–2016 period. It should be noted that the fire danger delivers an upward trend over most parts of South America, Canada, southeast and northeast United States, central Eurasia, and northern Russia, with potential implications to the Arctic environment. Less significant trends are seen in Australia and southern Africa. Negative trends indicating reduction in vegetation fire vulnerability are noticed over large parts of Asia and central Africa (e.g., Mali, Nigeria, Sudan, and Ethiopia) (Figure 3e). Turning to the *SD* analyses (Figure 3f), it is revealed that the PFIv2 variability is higher over central Africa and northern South America, which are regions with the highest intra-seasonal and interannual precipitation variability. Interestingly is that the extra-tropical region including the Artic, and the east

coast of North America (Figure 3f) show large *SD*. In eastern Australia, our results support the findings delivered by Mariani *et al.* (2016), insofar as fire danger variability is concerned.

In order to verify whether the PFIv2 reproduces the regions with higher concentration of satellite-derived hot spots, Figure 4 shows the capability of the PFIv2 model in locating the daily fires of the Terra/MODIS, coincident with the highest PFIv2 levels between 0.7 and 1. To verify if the use of ERAI precipitation can compromise the PFIv2 performance, we also show the PFIv2 calculation based on this dataset (Figure 4).

Africa is the continent with the highest fire occurrences on Earth. Figure 4a shows that 89% of the occurrence of fires fall within the PFIv2 highest classes (high and critical fire danger). Asia was the sub-region with lowest predominance of fires within those classes, 64% (Figure 4b). This may reveal that other drivers related to fire ignition/conditions play an important role in Asian fire activity, such as agricultural expansion and/or lightning. South America is characterized by a good match between fires and areas with the highest PFIv2 (Figure 4c), with values by about 72%. However, this is the region that presented the highest rate of fire occurrences in the minimum PFIv2 class. It should be noted that in case of fires located in low danger area is very unlike that these fires will evolve to erratic and intense wildfires.

The adjustment of PFIv2 to reproduce the fire susceptibility on extra-tropical latitudes, in particular over North America and Europe, demonstrates the efficiency of the method in detecting the potential for fire occurrences (Figure 4d,f). More than 65% of detected fires by MODIS occur in areas of PFIv2 higher than 0.7. It has to be stressed that analyses for Europe (Figure 4f) show that around 15% of the fire occurred in areas where atmospheric conditions are less susceptible to fires.

Regarding the Southwest Pacific region, which experiences an average of 150,000 fire occurrences during 2001–2016 period (Figure 2m,o), the PFIv2 shows an efficiency by up 75% in locating fires in the high and critical classes (Figure 4e). Local fires are highly dependent on the ignition material and litter that in some cases are not fully reproduced by the IGBP vegetation dataset used in our method. The vegetation file in the present study is static and does not take into account the temporal

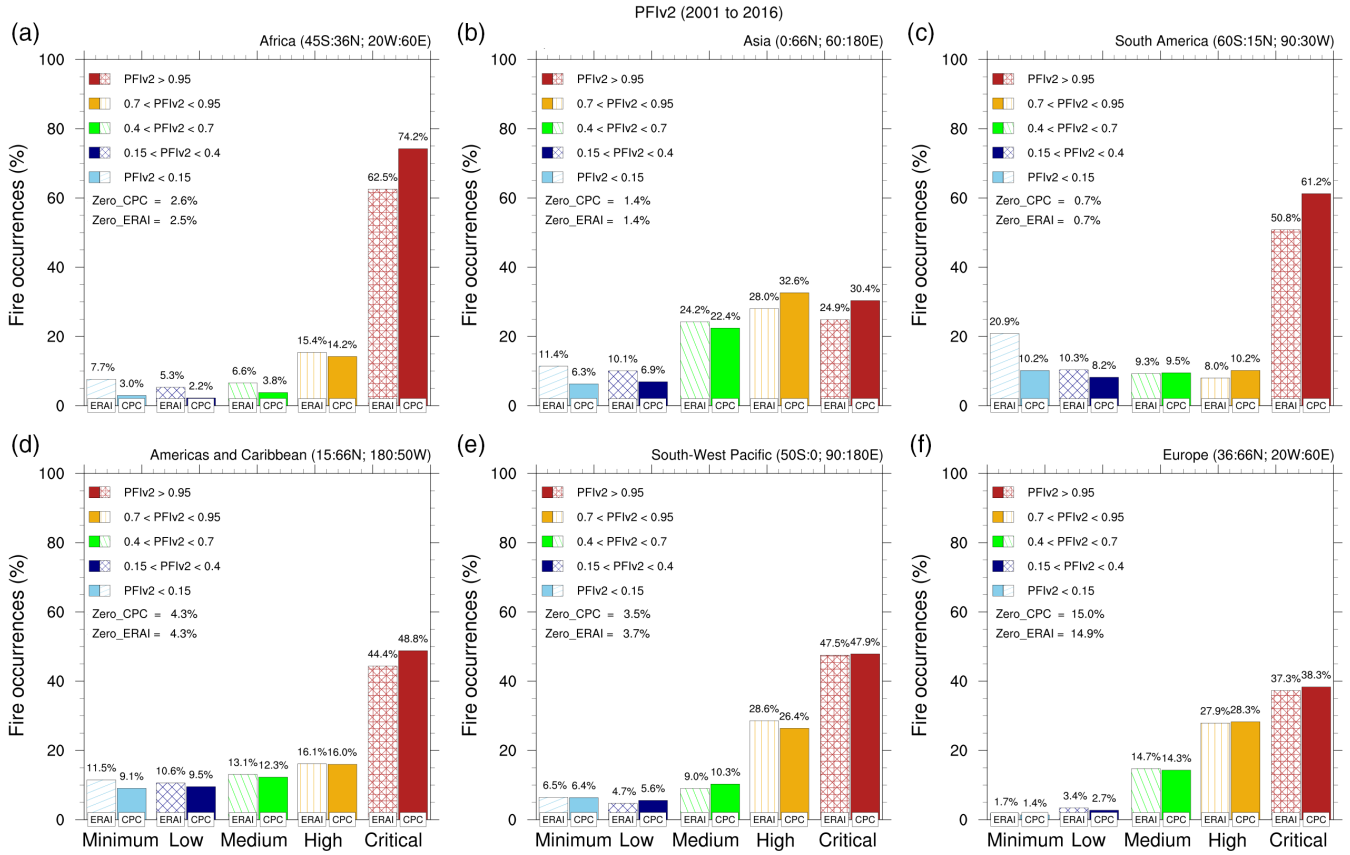

FIGURE 4 Percentage of daily accumulated fire at each PFIv2 class based on ERAI, and CPC precipitation dataset for the 2001–2016 period. (a) Africa, (b) Asia, (c) South America, (d) Americas and Caribbean, (e) South-West Pacific, and (f) Europe

variation of the land cover (seasonal or daily). For instance, the IGBP does not take into account increases in bushes/grasses underneath forests and savannas. Other aspect that should be mentioned is related to the fact that the IGBP grid does not include more than one vegetation type. This may reduce the fire danger by considering primary a larger area of green and well-watered vegetation.

Figure 5 provides the comparison between PFI and PFIv2 in representing the number of fires which falls within the fire danger classes. It is clear that most of fires are placed in the extreme (high and critical) fire danger, in particular from July to December. It is important to mention that the higher number of hot spots, by about 80%, occurs in the maximum levels of the PFIv2. In Asia, where fires do not occur predominantly in a specific period, detected fires fall in the high and critical categories covering up to 70% of the incidence. Large improvement is although noticed in Europe, for all season. Other

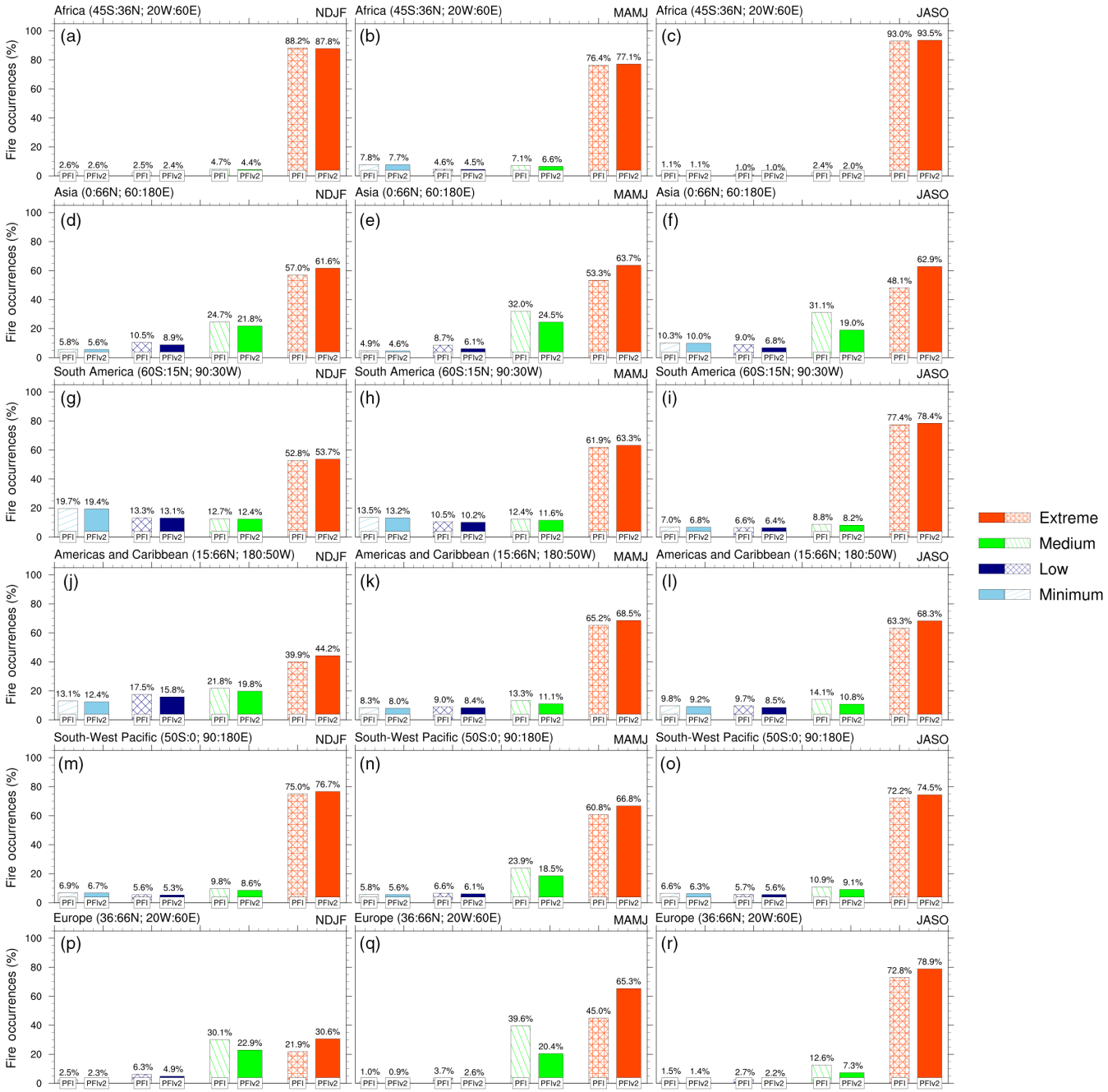

FIGURE 5 Distribution of seasonally satellite detected fires in the PFI, and PFIv2 fire danger classes for the 2001–2016 period. (a–c) Africa, (d–f) Asia, (g–i) South America, (j–l) Americas and Caribbean, (m–o) South-West Pacific, and (p–r) Europe. *Note:* Extreme level shows the sum of the high and critical fire danger classes

important aspect that should be highlighted is that the number of fires identified in the medium class in the PFI previous version is reduced in the PFIv2, in particular over Asia, and Europe.

As shown in Table 2, when all months are included the PFIv2 shows a better performance with respect to the PFI original version, in particular for Asia, Americas and Caribbean, and Europe. It might be highlighted that the modification in the temperature function and especially the inclusion of the LogHai parameterization has been responsible for improved performance.

Additional evaluation of the PFIv2 is conducted to verify its capability to reproduce burned areas (Figure 6). We have computed the spatial correlation between the fire danger index and burned area (BA) as delivered by the MODIS product available at University of Maryland ftp://fuoco.geog.umd.edu/MCD64CMQ/C6/. The dataset has been downloaded in 0.25° × 0.25° (latitude × longitude) grid covering the 2001–2016 interval. The BA is measured in hectares and high correlation indicates that large burned area fits properly with PFIv2 higher values. On the other hand, where correlation assumes lower values may indicate that small burned areas occurs within high PFIv2 and vice versa.

According to the global correlation pattern (Figure 6), correlation higher than 0.6 is observed in the fire activity preferential regions, namely South America and Africa. Reasonable match between the PFIv2 and BA is also noted in the Pacific islands and northern Australia, southern Asia and central Eurasia. The size of burned area is dependent primarily on the fire intensity and the amount of combustible material. Thus, in some areas despite high fire danger the severity of burning is limited. This is very usual in periods followed by intense fire activity in the previous year. Another aspect that interferes in the correlations values is related to the grid size of the PFIv2. Because it contains only the dominant vegetation class, whereas in reality the same grid may be covered by mixed vegetation which can include grassland and shrubs, which in case of fires would favour an increase in the burned area.

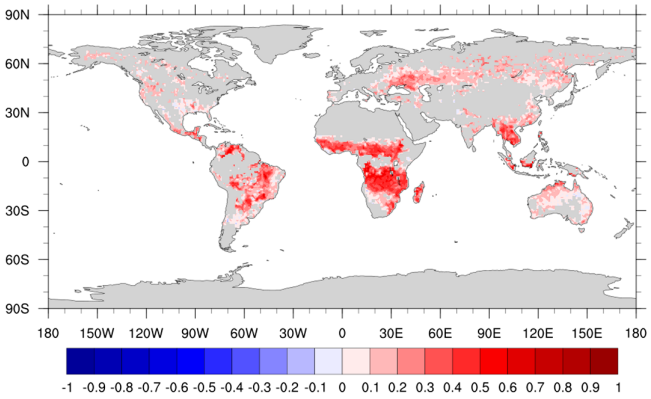

FIGURE 6 Correlation between the PFIv2 and burned areas (MODIS product) in the 2001–2016 interval

4 | SEASONALITY OF THE PFIV2

To evaluate the fire danger in a single seasonal interval over the entire globe for some regions does not show a particular characteristic, and may overlook important features. For example, in the 'south-west pacific region', northern and southern Australia have very different peak fire seasons (June–July peak in the north, December–January peak in the south). Similarly occurs in South America, whereas the Northern Hemisphere part shows more fires from January to March. To provide an evaluation of the PFIv2 annual cycle, it is calculated the first harmonic of Fourier transform which can provide spatial information on the amplitude of the annual cycle, the month with the highest fire danger and the explained variance. Harmonic analysis characterizes dominant features in the time–space domain (Justino *et al.*, 2011). The first order harmonics of meteorological parameters deliver long-term effects (annual cycle), while higher order harmonics are related to short-term fluctuations (intra-seasonal). The phase angle can be used to determine the time when the maximum or minimum of a given harmonic occurs. Thus, the phase angle is very useful to identifying the month with the maximum occurrence of the fire danger.

TABLE 2 Percentage of daily detected hot spots/fires found within the PFI and PFIv2 high and critical classes (≥0.7) for the 2001–2016 period

Region (WMO)	PFI_Max (%)	PFIv2_Max (%)	PFIv2 – PFI (%)
Africa	87.9	88.4	+0.5
Asia	52.8	63	+10.2
South America	70.4	71.4	+1.0
Americas and Caribbean	60.8	64.8	+4.0
South-West Pacific	71.7	74.3	+2.6
Europe	55.1	66.6	+11.5

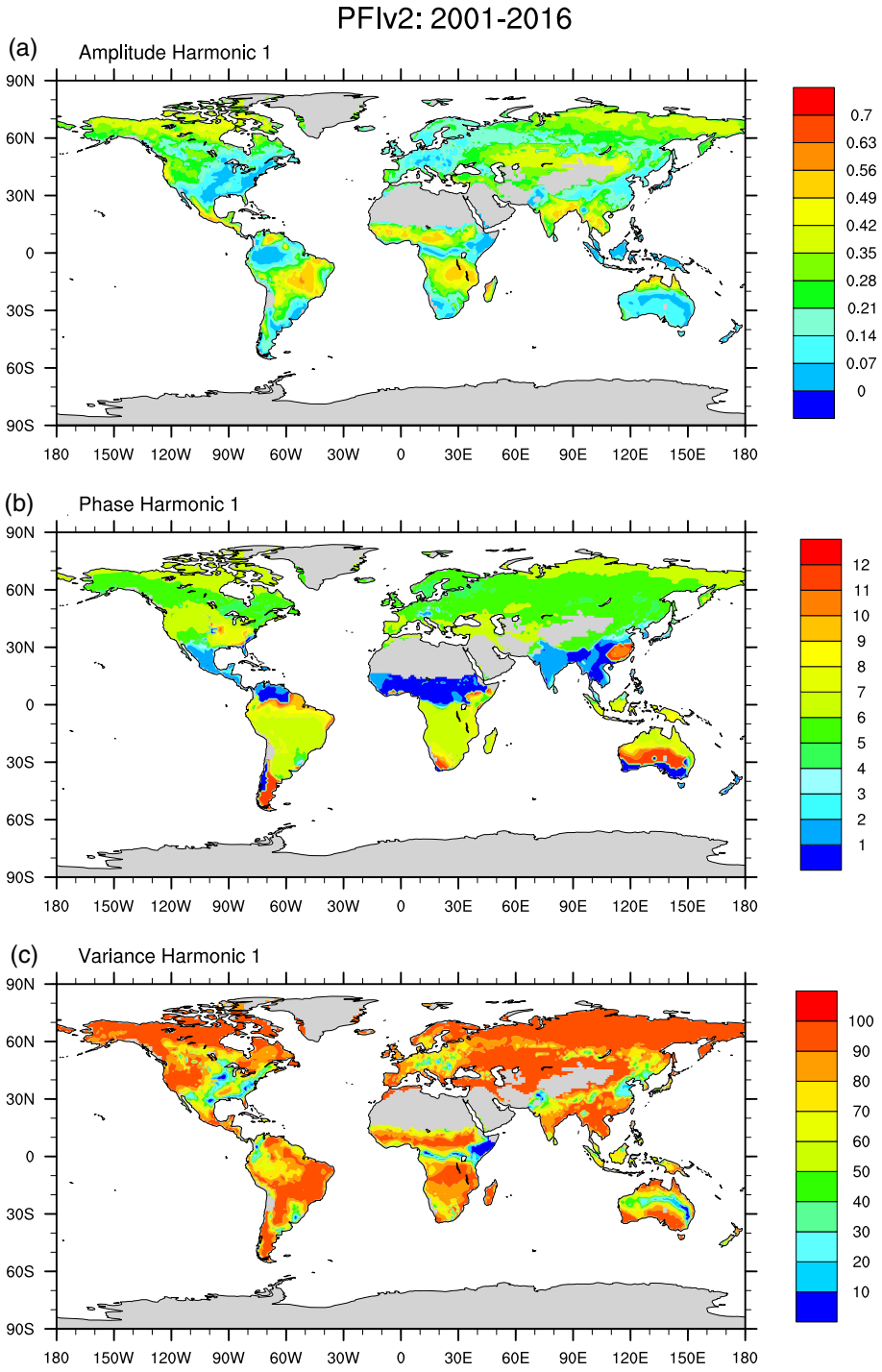

FIGURE 7 Harmonic analyses of PFIv2. (a) Amplitude of the annual cycle or first harmonic, (b) the phase of the first harmonic (month), and (c) shows the explained variance of the first harmonic (%)

As shown in Figure 7a, Africa and South America experience a dominant season also shown in northern Australia and southern Asia. In Africa two regions of maxima amplitude are identified, which are related with the annual migration of the Intertropical Convergence Zone, and associated semi-annual dry season. Larger amplitude is also noted in the Arctic region of east Asia and Canada corroborating with the fire season peak in July. Based on Figure 7b is clear that higher fire danger in the Southern Hemisphere is concentrated between July and October, whereas in the Northern Hemisphere due to climate diversity, fire danger shows regional patterns. By analysing, the variance (Figure 7c) is clear that in some regions the seasonal cycle is not dominant (e.g., central Europe, Australia and Africa, Mexico and southern North America). This indicates that the fire danger and hot spots can occur throughout the year, with perhaps peaks dominated by the semi-annual component or higher order harmonics.

5 | CONCLUDING REMARKS

Based on the second version of the Potential Fire Index (PFIv2), this study evaluates the interannual variability of vegetation fires and the global susceptibility to the fire occurrences. It is demonstrated that proposed modification in the PFIv2 properly reproduces the regions with the highest incidence of fires in Asia, North America and Europe. The PFIv2 was also compared to burned areas based on MODIS product between 2001 and 2016.

Although the adjustment prioritizes the extra-tropical regions, the model was also efficient in reproducing high susceptibility to fire occurrences over other regions. Modification of the air temperature factor from a latitudinal adjustment and the Haines logarithmic function, to take into account the surface elevation, demonstrated that the PFIv2 locates fires which are located in vulnerable and higher danger zones in 88.4% of the cases. The efficiency of the PFIv2 in reproducing regions with fire susceptibility was also demonstrated in Asia. Only the high and critical classes of the model accounted for more than half of the incident fires (63%), based on CPC precipitation data. The PFIv2 also matches the MODIS burned areas with correlations higher than 0.6 over the most susceptible regions such as Africa and South America, slightly lower correlation are found where fire does not primary follows the climate annual cycle, and is dominated by high frequency events.

The PFIv2 shows some caveats due to the high dependence of the days of dryness, which is computed from the precipitation data. Currently, estimates of precipitation are still a very complex task in a global domain due to the lack of observations, and also presents divergences among the atmospheric models and reanalyses data. However, it was demonstrated that the CPC data is more reasonable than the ERAI dataset, which tends to overestimate the daily precipitation. Future improvements of the PFIv2 are still needed and should incorporate a better representation of vegetational changes, the inclusion of lightning and density population function, for instance. Although the results presented here are based solely on atmospheric vulnerability, it may be argued that regardless of the source of ignition climatic factors are primordial for the fire occurrences.

ACKNOWLEDGEMENTS

The authors acknowledge the support of the Coordination for the Improvement of Higher Education Personnel (CAPES), the Minas Gerais Research Foundation (FAPEMIG), and the Brazilian National Council for Scientific and Technological Development (CNPq). We are also grateful to the Federal University of Western Para (Ordinance N° 594, of March 4, 2015); to the Graduate Program in Applied Meteorology of the Federal University of Vicosa (www.posmet.ufv.br), and to the Fire Program of the National Institute of Space Research – Brazil (INPE). We are very thankful to Cristian F. Zuluaga for processing the area burned dataset.

ORCID

Alvaro Avila-Diaz https://orcid.org/0000-0002-0404-4559

REFERENCES

Andrews, P.L. and Bradshaw, l.S. (1997) Fires: Fire Information Retrieval and Evaluation System – A Program for Fire Danger Rating Analysis. General Technical Report (GTR). INT-GTR-367. Ogden, UT: U. S. Department of Agriculture, Forest Service, Intermountain Research Station, 64 p.

Anjos, L.J.S. and de Toledo, P.M. (2018) Measuring resilience and assessing vulnerability of terrestrial ecosystems to climate change in South America. *PLoS One*, 13(3), e0194654. https://doi.org/10.1371/journal.pone.0194654.

Archibald, S., Roy, D.P., Van Wilgen, B.W. and Scholes, R.J. (2009) What limits fire? An examination of drivers of burnt area in southern Africa. *Global Change Biology*, 15, 613–630.

Bradstock, R.A. (2010) A biogeographic model of fire regimes in Australia: current and future implications. *Global Ecology and Biogeography*, 19, 145–158. https://doi.org/10.1111/j.1466-8238.2009.00512.x.

Burgan, R.E. (1988) Revisions to the 1978 National Fire Danger Rating System. Res. Paper SE-273. Asheville, NC: U. S. Department of Agriculture, Forest Service, Southeastern Forest Experiment Station.

Catchpole, W. (2002) In: Bradstock, R.A., Williams, J.E. and Gill, A. M. (Eds.) *Fire Properties and Burn Patterns in Heterogeneous Landscapes. Flammable Australia: The Fire Regimes and Biodiversity of a Continent*. Cambridge: Cambridge University Press, pp. 50–75.

Dee, D.P., Uppala, S.M., Simmons, A.J., Berrisford, P., Poli, P., Kobayashi, S., Andrae, U., Balmaseda, M.A., Balsamo, G., Bauer, P., Bechtold, P., Beljaars, A.C.M., van de Berg, L., Bidlot, J., Bormann, N., Delsol, C., Dragani, R., Fuentes, M., Geer, A.J., Haimberger, L., Healy, S.B., Hersbach, H., Hólm, E. V., Isaksen, L., Kållberg, P., Köhler, M., Matricardi, M., McNally, A.P., Monge-Sanz, B.M., Morcrette, J.J., Park, B.K., Peubey, C., de Rosnay, P., Tavolato, C., Thépaut, J.N. and Vitart, F. (2011) The ERA-interim reanalysis: configuration and performance of the data assimilation system. *Quarterly Journal of the Royal Meteorological Society*, 137(656), 553–597.

Fetter, R., Carlos, H. and Steinke, E. (2018) Um Índice para Avaliação da Variabilidade Espaço-Temporal das Chuvas no Brasil. *Revista Brasileira de Meteorologia*, 2, 225–237.

Finney, M.A., Cohen, J.D., Mcallister, S.S. and Jolly, W.M. (2012) On the need for a theory of wildland fire spread. *International Journal of Wildland Fire*, 22(1), 25–36.

Friedl, M.A., Sulla-Menashe, D., Tan, B., Schneider, A., Ramankutty, N., Sibley, A. and Huang, X. (2010) MODIS collection 5 global land cover: algorithm refinements and

characterization of new datasets. *Remote Sensing of Environment*, 114, 168–182.

Giglio, L., Schroeder, W. and Justice, C. (2016) The collection 6 MODIS active fire detection algorithm and fire products. *Remote Sensing of Environment*, 178, 31–41. https://doi.org/10.1016/j.rse.2016.02.054.

Haines, D.A. (1988) A lower atmosphere severity index for wildland fires. *National Weather Digest*, 13, 23–27.

Harrison, S.P., Power, M. and Bond, W. (2007) Paleofires and the Earth system. *iLEAPS Newsletter*, 3, 18–20.

Hickler, T., Prentice, I.C., Smith, B., Sykes, M.T. & Zaehle, S., et al. (2006) Implementing plant hydraulic architecture within the LPJ dynamic global vegetation model. *Global Ecology and Biogeography*, 15(6), 567–577. https://doi.org/10.1111/j.1466-8238.2006.00254.x.

Hollmann, R., Merchant, C., Saunders, R., Downy, C., et al. (2013) The ESA climate change initiative: satellite data records for essential climate variables. *Bulletin of the American Meteorological Society*, 94, 1541–1552.

Huang, X., Rein, G. and Chein, H. (2015) Computational smoldering combustion: predicting the roles of moisture and inert contents in peat wildfires. *Proceedings of the Combustion Institute*, 35, 2673–2681.

Huffman, G.J., Adler, R.F., Arkin, P., Chang, A., Ferraro, R., Gruber, A., Janowiak, J., McNab, A., Rudolf, B. and Schneider, U. (1997) The global precipitation climatology project (GPCP) combined precipitation dataset. *Bulletin of American Meteorological Society*, 78, 5–20. https://doi.org/10.1175/1520-0477(1997)078<0005:TGPCPG>2.0.CO;2.

Justino, F., Melo, A.S., Setzer, A., Sismanoglu, R., Sediyama, G.C., Ribeiro, G.A., Machado, J.P. and Sterl, A. (2010a) Greenhouse gas induced changes in the fire risk in Brazil in ECHAM5/MPI-OM coupled climate model. *Climatic Change*, 106(2), 285–302.

Justino, F., Peltier, W. and Barbosa, H. (2010b) Atmospheric susceptibility to wildfire occurrence during the last glacial maximum and mid-Holocene. *Palaeogeography, Palaeoclimatology, Palaeoecology*, 295, 76–88. https://doi.org/10.1016/j.palaeo.2010.05.017.

Justino, F., Setzer, A., Bracegirdle, T.J., Mendes, D., Grimm, A., Dechiche, G. and Schaefer, C.E.G.R. (2011) Harmonic analysis of climatological temperature over Antarctica: present day and greenhouse warming perspectives. *International Journal of Climatology*, 31, 514–530. https://doi.org/10.1002/joc.2090.

Justino, F., Stordal, F., Clement, A., Coppola, E., Setzer, A. and Brumatti, D. (2013) Modelling weather and climate related fire risk in Africa. *American Journal of Climate Change*, 2, 209–224.

Krause, A., Kloster, S., Wilkenskjeld, S. and Paeth, H. (2014) The sensitivity of global wildfires to simulated past, present, and future lightning frequency. *Journal of Geophysical Research: Biogeosciences*, 119, 312–322. https://doi.org/10.1002/2013JG002502.

Langmann, B., Duncan, B., Textor, C., Trentmann, J. and van der Werf, G.R. (2009) Vegetation fire emissions and their impact on air pollution and climate. *Atmospheric Environment*, 43(1), 107–116.

Leys, B.A., Marlon, J.R., Umbanhowar, C. and Vannière, B. (2018) Global fire history of grassland biomes. *Ecology Evolution*, 8, 8831–8852. https://doi.org/10.1002/ece3.4394.

Mariani, M., Fletcher, M.-S., Holz, A. and Nyman, P. (2016) ENSO controls interannual fire activity in southeast Australia. *Geophysical Research Letters*, 43, 10891–10900. https://doi.org/10.1002/2016GL070572.

Marlier, M.E., DeFries, R.S., Voulgarakis, A., Kinney, P.L., Randerson, J.T., Shindell, D.T., Chen, Y. and Faluvegi, G. (2013) El Niño and health risks from landscape fire emissions in southeast Asia. *Nature Climate Change*, 3(2), 131–136.

Masrur, A., Petrov, S.N. and Degroote, J. (2018) Circumpolar spatio-temporal patterns and contributing climatic factors of wildfire activity in the Arctic tundra from 2001–2015. *Environmental Research Letters*, 13, 014019. https://doi.org/10.1088/1748-9326/aa9a76.

Murdiyarso, D. and Adimingsih, E.S. (2007) Climate anomalies, Indonesian vegetation fires and terrestrial carbon emissions. *Mitigation and Adaptation Strategies for Global Change*, 12, 101–112. https://doi.org/10.1007/s11027-006-9047-4.

Page, S.E., Siegert, F., Rieley, J.O., Boehm, H.D.V., Jaya, A. and Limin, S. (2002) The amount of carbon released from peat and Forest fires in Indonesia during 1997. *Nature*, 420, 61–65. https://doi.org/10.1038/nature01131.

Pereira, M.P.S., Justino, F., Malhado, A.C.M., Barbosa, H. and Marengo, J. (2014) The influence of oceanic basins on drought and ecosystem dynamics in Northeast Brazil. *Environmental Research Letters*, 9(12), 124013.

Potter, B. (2018) The Haines Index – it's time to revise it or replace it. *International Journal of Wildland Fire*, 27(7), 437–440. https://doi.org/10.1071/WF18015.

Reboita, M.S., Gan, M.A., Rocha, R.P. and Ambrizzi, T. (2010) Regimes de precipitação na América do Sul: uma revisão bibliográfica. *Revista Brasileira de Meteorologia*, 25(2), 185–204.

Scheiter, S. and Higgins, S.I. (2009) Impacts of climate change on the vegetation of Africa: an adaptive dynamic vegetation Modelling approach. *Global Change Biology*, 15(9), 2224–2246.

Serreze, M.C. and Barry, R.G. (2010) Climate change. In: Barry, R. G. and Chorley, R.J. (Eds.) *Atmosphere. Weather and Climate*. Oxon: Routledge.

Silva, J.M.N., Pereira, J.M.C., Cabral, A.I., Vasconcelos, M.J.P., Mota, B. and Gregoire, J.M. (2003) An estimate of the area burned in southern Africa during the 2000 dry season using SPOT-VEGETATION satellite data. *Journal of Geophysical Research*, 108(D13), 8498.

Silva Junior, C.H.L., et al. (2019) Fire responses to the 2010 and 2015/2016 Amazonian droughts. *Frontiers in Earth Science*, 7, 97.

Skinner, D.J., Rocks, S.A. and Pollard, S.J. (2014) A review of uncertainty in environmental risk: characterising potential natures, locations and levels. *Journal of Risk Research*, 17(2), 195–219.

Sopko, P., Bradshaw, l. and Jolly, M. (2016) Spatial products available for identifying areas of likely wildfire ignitions using lightning location data-Wildland Fire Assessment System (WFAS). In: 6th International Lightning Meteorology Conference, 20–21 April 2016, San Diego, California, USA.

Sun, Q., Miao, C., Duan, Q., Ashouri, H., Sorooshian, S. and Hsu, K.L. (2018) A review of global precipitation data sets: data sources, estimation, and intercomparisons. *Reviews of Geophysics*, 56(1), 79–107.

Tymstra, C., Bryce, R.W., Wotton, B.M., Taylor, S.W. and Armitage, O.B. (2010) Development and Structure of

Prometheus: The Canadian Wildland Fire Growth Simulation Model. Natural Resources Canada, Information Report NOR-X-417. Canadian Forest Service, Northern Forestry Centre.

Van Wagner, C.E. (1970) Conversion of William's Severity Rating for Use with the Fire Weather Index. Information Report PS-X-21. Ontariom, Canada: Canadian Forestry Service.

Van Wagner, C.E. (1987) Development and Structure of the Canadian Forest Fire Weather Index System. Forest Technology Report, v. 35. Ottawa: Canadian Forestry Service.

Veraverbeke, S., Rogers, B.M., Goulden, M.L., Jandt, R., Miller, C. E., Wiggins, E. & Randerson, J.T. & , et al. (2017) Lightning as a major driver of recent large fire years in North American boreal forests. *Natural Climate Change*, 7, 529–534. https://doi.org/10.1038/nclimate3329.

Warmink, J., Janssen, J., Booij, M.J. and Krol, M.S. (2010) Identification and classification of uncertainties in the application of environmental models. *Environmental Modelling & Software*, 25(12), 1518–1527.

Williams, D.E. (1959) Fire Season Severity Rating. Technical Note No. 73. Department of Northern Affairs and National Resources, Forest Research Division, pp. 13.

Winkler, J.A., Potter, B.E., Wilhelm, D., Shadbolt, R.P., Piromsopa, K. and Bian, X. (2007) Climatological and statistical characteristics of the Haines index for North America. *International Journal of Wildland Fire*, 16, 139–152. https://doi.org/10.1071/WF06086.

Wolfson, R. (2012) *Energy, Environment and Climate*, 2nd edition. New York: WW Norton and Company, pp. 366–370.

Wooster, M.J. and Zhang, Y.H. (2004) Boreal forest fires burn less intensely in Russia than in North America. *Geophysical Research Letters*, 31(20), L20505. https://doi.org/10.1029/2004GL020805.

Xie, P., Chen, M. and Shi, W. (2010) 2.3A CPC unified gauge-based analysis of global daily precipitation. Preprints. In: 24th Conference on Hydrology. American Meteorological Society [Online]. Available at: https://ams.confex.com/ams/90annual/webprogram/Paper163676.html [Accessed 25th July 2019].

How to cite this article: da Silva AS, Justino F, Setzer AW, Avila-Diaz A. Vegetation fire activity and the Potential Fire Index (PFIv2) performance in the last two decades (2001–2016). *Int J Climatol*. 2021;41 (Suppl. 1):E78–E92. https://doi.org/10.1002/joc.6648